Mixing dynamics in double-diffusive convective stratified fluid layers

Rishabh More[1] and Sridhar Balasubramanian[1,2,*]

[1]Department of Mechanical Engineering, and
[2]Interdisciplinary Programme in Climate Studies,
Indian Institute of Technology Bombay, Mumbai 400 076, India

Double-diffusive convection in a linearly stratified fluid in the presence of radiative cooling at the surface has been investigated experimentally and theoretically. The stratification strength, which was varied in the experiments, is characterized by the buoyancy frequency of a stable environment defined as $N^2 = (g/\rho_0)/(d\rho/dz)$. The surface radiative cooling mimics buoyancy forcing incumbent at the surface of the ocean during the boreal winter months. The significant parameters governing the mixing dynamics for such a system were identified to be the Richardson number (*Ri*) and flux Rayleigh number (Ra_f). Controlled experiments were performed for $Ri = 0$–6, while maintaining a constant $Ra_f = 2.58 \times 10^7$. This indicates that the stratification strength *N* was changed while the cooling flux $\dot{Q}$ was fixed. The mixing and barrier layers were visualized using a commercial dye solution. The thickness of the mixing layer was quantified from the flow evolution images. It was found that the mixing layer decays exponentially with increase in the stratification strength owing to suppression of downward convective motion due to the buoyancy force. A similar trend was observed for the entrainment velocity. A scaling law was proposed as follows: $\Delta = CRi^{-3/4}$, where Δ is the mixing layer depth and *C* is a constant. The experimental results were compared with theoretical analysis and reasonable agreement was found. The results would be useful in parameterizing the mixing and barrier layers in strongly stratified environments such as the Bay of Bengal.

Keywords: Double-diffusive convection, entrainment velocity, linear stratification, radiative cooling, mixing layer depth.

DOUBLE-DIFFUSIVE convection is driven by two different density gradients that diffuse at different rates[1]. The density gradients in a fluid drive the process of convection, since density gradient gives rise to buoyancy variation that initiates the process of convection. The density gradients may arise from of variations in the composition of the fluid or variations in temperature. A common example of double-diffusive convection is in oceanography, where temperature (in the form of heat or cooling flux) and salt concentration (salinity) exist with different gradients and diffuse at differing rates. A mechanism that affects both these variables is the input of cold freshwater from icebergs or rivers. This diffusion depends on the relative magnitude of the rate of diffusion of salinity and temperature. In general, temperature diffuses faster than salinity by around two orders of magnitude.

Double-diffusive convection is important in understanding the evolution of a number of systems that have multiple causes for density variations. These include convection in the earth's oceans (as mentioned above), in magma chambers, and in the sun (where heat and helium diffuse at differing rates). The importance of double-diffusion in oceanic events is becoming widely accepted, in part due to the understanding of phenomena such as the role of salt fingering in determining the temperature–salinity relationship in the mid-latitudes[1] and maintenance of the marginal ice edge by heat transport through a diffusive interface[2].

Turner and Stommel[3] were the first to perform laboratory demonstrations on the formation of a series of convecting layers separated by thin stable density interfaces when a stably stratified fluid with respect to salt is heated from below. This has inspired researchers in recent decades to investigate the double-diffusive convection phenomenon using laboratory experiments[4–8] and *in situ* observations[9–12]. The laboratory experiments mostly studied the formation of convective layers in a stratified fluid heated from below, where the convecting layer at the bottom had the largest thickness and the other layers (referred to as subsequent layers hereafter) had comparable thicknesses. A differential model for salt-stratified double-diffusive systems, heated from below, was presented by Bergman *et al.*[13]. Turner[4] suggested that the mixing at the front of the double-diffusive instability was in the form of Rayleigh–Taylor instability. Based on the argument that the entrainment interface is marginally stable and utilizing conservation equations for temperature and salinity, Turner[4] proposed that $\alpha \Delta T = \beta \Delta S$, where ΔT and ΔS are the temperature and salinity difference across the interface, and α and β are the coefficients of thermal expansion and saline contraction respectively. Upon applying a heat flux (or cooling flux), $\dot{Q}$, from bottom (top) and using the conservation equations for temperature and salinity, it was proposed that the mixed layer depth (MLD), Δ, takes the form

$$\Delta = CQ^{1/2}N^{-1}t^{1/2}, \quad (1)$$

where Q is the buoyancy flux related to the cooling flux given by

$$Q = \frac{\alpha g \dot{Q}}{\rho_0 C_p}$$

with ρ_0 being the reference density, C_p the specific heat and g is the acceleration due to gravity. In eq. (1), C is a constant, which was found to vary between 1.06 and 1.63.

*For correspondence. (e-mail: sridharb@iitb.ac.in)

Turner[4] indicated that as the mixing layer develops, a thermal boundary layer forms at the top of the mixed layer due to escape of heat. The final analysis showed that the thickness of MLD should take the form

$$\Delta = \left(\frac{1}{4}R_c\right)^{1/4}\left(\frac{\nu Q^{1/3}}{k^2 N^8}\right)^{1/4}, \tag{2}$$

where R_c is the critical Rayleigh number at which the thermal boundary layer becomes unstable, ν the kinematic viscosity of the fluid and k is the thermal conductivity of the fluid. From the experimental results of Newman[14], it was deduced that the critical Rayleigh number took a value of $\sim 2.4 \times 10^4$, which was an order of magnitude higher than the expected theoretical value of $R_c = 10^3$ proposed from the theory[15].

Fernando[6] provided a new dimension to this problem by considering the fact that the dynamics of double-diffusive convection is controlled by turbulent entrainment rather than Rayleigh–Taylor instability as assumed by Turner[4]. It was postulated that the entrainment is manifested by the engulfment of non-turbulent fluid by the integral eddies near the interface. Such an entrainment mechanism is akin to that observed by Deardorff *et al.*[16]. Therefore, an entrainment hypothesis was used to estimate Δ. The hypothesis assumes that the entrainment rate is related to the rate of change of potential energy, λ as follows

$$\frac{\mathrm{d}\lambda}{\mathrm{d}t} = \frac{1}{4}\rho_0 N^2 h^2 \frac{\mathrm{d}h}{\mathrm{d}t}. \tag{3}$$

The entrainment law states that the rate of change of potential energy is proportional to the kinetic energy flux, available at the interface, which gives

$$\frac{1}{4}\rho_0 N^2 h^2 \frac{\mathrm{d}h}{\mathrm{d}t} = \underline{\alpha}(\overline{w^2})^{3/2}, \tag{4}$$

where $\underline{\alpha}$ is the entrainment coefficient, $(\overline{w^2})^{1/2}$ the RMS velocity near the interface and h is the mixing depth.

The critical depth of the mixed layer, Δ, can be found using the parameterization for the RMS velocity at any height h within the convective boundary layer[17] given by

$$(\overline{w^2})^{1/2} = C_1(Qh)^{1/3}, \tag{5}$$

along with the equation[18],

$$\overline{w^2} = C_2 \delta b \Delta, \tag{6}$$

where $\delta b = C_3 N^2 \Delta$ is the buoyancy jump and C_1, C_2, C_3 are proportionality constants. The final equation for Δ takes the form

$$\Delta = C_4\left(\frac{Q}{N^3}\right)^{1/2}, \tag{7}$$

with the constant $C_4 = (C_1^2/C_2C_3)^{3/4}$.

Although the dynamics may be similar, relatively few studies have been conducted for the case when instead of heating from below the stratified fluid is cooled from the top. Here, the faster diffusion of cooling flux gives rise to mixed layer at the top and the mixing is typically restricted to a finite depth, Δ, beyond which cooling flux cannot penetrate due to the opposing buoyancy offered by the salinity gradient. In steady state, all the properties such as salinity and temperature (and as a result density) are constant within the mixed layer. Below the mixed layer exists the small barrier layer, which separates the mixed layer and the deep cold water. Strong temperature and salinity gradients exist in the barrier layer and thickness of this layer is called the barrier layer depth (BLD). Below the BLD, the fluid properties follow a smooth variation as if not affected by the flux and the associated mixing. The barrier layer formation was not documented by Fernando[6]. Furthermore, a staircase-like mixing layer profile was seen by him[6], which is a consequence of heating from the bottom. We do not expect such staircase profiles in the present study, but an evident mixed layer and barrier layer profiles would be seen because of cooling from the top.

One of the applications of double-diffusive mixing due to cooling from the top is in the Bay of Bengal (BoB), where a strong near-surface stratification exists naturally due to the huge freshwater influx from the Ganges[19]. In the BoB, sea surface temperature (SST) anomalies play a pivotal role in the evolution of atmospheric events[20] (e.g. monsoon system, formation of cyclones, etc.). In turn, SST anomalies are driven by the processes responsible for the heat budget and thickness of the mixed layer[11] (e.g. energy fluxes through the sea surface, horizontal and vertical advection). An empirical relation of the MLD with cooling flux and stratification in the BoB would provide crucial information on the mean and time-varying SST dynamics in a region of important air–sea interactions.

Due to the presence of freshwater layer over deep cold water, coupled with sub-seasonal monsoon oscillations, even a small change in the ocean surface conditions may affect the mixing dynamics and result in tropical cyclones, diurnal cycles, monsoon disturbances, etc. A thin mixing layer indicates that temperature cannot penetrate deeper into the ocean and that deeper colder water does not come up. This affects the ocean surface temperature, which in turn affects the convection in the immediate atmosphere boundary layer. This feedback is important in predicting monsoon and formation of cyclones. So, studying mixing dynamics in double-diffusive stratified fluids is important in understanding the effect of temperature on the mixing dynamics in BoB.

Given the application of double-diffusive mixing in BoB and the importance of understanding the underlying physics, the objective of this study is to examine the phenomenon of mixing in stratified systems in a laboratory framework. Initially, a dimensional analysis of the mixing dynamics problem was done to identify the parameters important in mixing in the stratified double-diffusive systems. Experiments were performed to quantify density (ρ), temperature (T), salinity (S) and cooling flux, and the effect of changing these parameters on MLD and entrainment velocity. In the present study, for linear stratification, we probe the lower ranges of N to examine the applicability of eq. (7). Along with the formulation for mixed layer thickness, the vertical profiles of density are also presented to demarcate the mixed layer and barrier layer, and to relate them to the vertical oceanic structure. Lastly, a parameterization for entrainment velocity, U_e, is also developed.

A range of parameters governs the dynamics of double-diffusive convection. Here we explore these parameters and using physical arguments form a set of important non-dimensional parameters. For double-diffusive convection in a 2D configuration, the important dimensional parameters are the buoyancy flux imposed on the surface (Q), total height of the fluid layer (H), reference density (ρ_0), vertical gradient of density ($\mathrm{d}\rho/\mathrm{d}z$), gravity ($g$), thermal diffusivity of the fluid (K_T), specific heat of fluid (C_p), thermal conductivity of the fluid (K), kinematic viscosity (ν) and thermal coefficient of expansion of the fluid (α). Any external parameter, e.g. mixing length Δ or entrainment velocity U_e, can be written as a function of the above-mentioned parameters as follows

$$\Delta = F\left(Q, H, \rho_0, \frac{\mathrm{d}\rho}{\mathrm{d}z}, g, K_\mathrm{T}, C_p, K, \nu, \alpha\right).$$

If the effect of planetary rotation, which is common in geophysical flows, were to be considered in the above analysis, then the Coriolis parameter 2Ω would be present. After application of the Buckingham–Pi theorem, six π terms should remain in the final expression. The above equation can be rewritten as

$$\Delta = F(Q, H, N, K_\mathrm{T}, C_p, K, \nu, \alpha),$$

where $N = \sqrt{(-g/\rho_0)(\mathrm{d}\rho/\mathrm{d}z)}$ is the buoyancy frequency. With the help of physical arguments, it can be shown that the above equation reduces to

$$\Delta^* = F(Ra_f, Ri, Re, Pr, Pe),$$

where $\Delta^* = \Delta/H$ is the non-dimensional thickness representing the MLD, $Ra_f = QH^3/WK_\mathrm{T}\nu$ the flux Rayleigh number which scales buoyancy to viscous effects in mixing, $Ri = N^2H^2/W^2$ the Richardson number that expresses buoyancy to inertia effects in mixing, $Re = WH/\nu$ the Reynolds number, which is ratio of inertial to viscous forces in mixing, $Pr = \nu/k_T$ is the Prandtl number, which is ratio of momentum diffusivity to thermal diffusivity, $Pe = WH/k_T$ is Peclet number that scales advective transport rate to diffusive transport rate. Here, W is the velocity scale given by $W = (QH)^{1/3}$.

It can be inferred from the above analysis that a non-dimensional mixing length-scale Δ^* primarily depends on four non-dimensional parameters, viz. Re, Ri, Pe and Ra_f. In our experiments, Pr is a constant.

$$\Delta^* = F(Re, Ri, Pe, Ra_f). \tag{8}$$

The main objective of the experiments is to generate a double-diffusive stratified environment to mimic conditions in BoB and study the mixing dynamics when it is cooled from the top to check the validity of eq. (7) for low Richardson number cases. The experiments were conducted in a tank that was 90 cm long, 30 cm wide and 48 cm high. The linear stratification was obtained using the standard two-tank technique of Oster and Yamamoto[21]. This technique utilizes two overhead tanks; with tank T1 containing water–salt mixture with maximum density required and tank T2 containing freshwater. The valves V1 and V2 were opened at the same time and the mixture in tank (T1) was stirred continuously in order to ensure uniform mixing. Density was measured using a densitometer. The fluid was drawn with syringes installed at different heights (z) and then fed into the densitometer. The stratification strength $N = \sqrt{(-g/\rho_0)/(\mathrm{d}\rho/\mathrm{d}z)}$ as a measure of stratification was used. It was observed that except at the bottom and top of the tank, an excellent linear stable stratification profile was obtained. Such behaviour is expected given the no flux boundary condition at the two boundaries, where gradients adjust to a zero value. The stability frequencies based on the two procedures agreed within ± 5%. Figure 1 shows the experimental set-up.

The cooling flux was provided with the help of commercial ice contained in an aluminum tray that was kept in contact with the top surface of water during the experiment. The cooling flux was calculated by applying Fourier's law across the bottom surface of the tray, since temperature gradient across the bottom plate was observed to be constant for a fixed amount of ice in the tray. It was observed that 10 kg of ice insulated from all sides, except the bottom of the tray, gives a cooling flux of $\dot{Q} \approx 1$ kW/m^2. The associated measurement uncertainties were estimated to be within ±5%. Temperature was measured by drawing out water at different depths using a syringe. The experiments were begun by placing the aluminum tray filled with ice in contact with the top surface of the stratified fluid. The mixing was visualized with the help of commercial dye. Initially, the mixing height was observed to increase at a fast rate for the first few

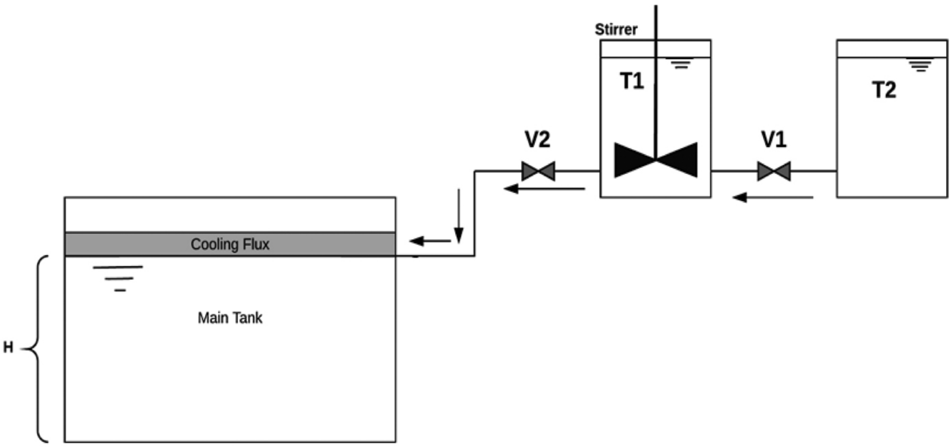

Figure 1. Experimental set-up. Tank T1 contains a salt–water mixture, tank T2 contains freshwater. V1 and V2 are valves. The total height of the tank is given by H.

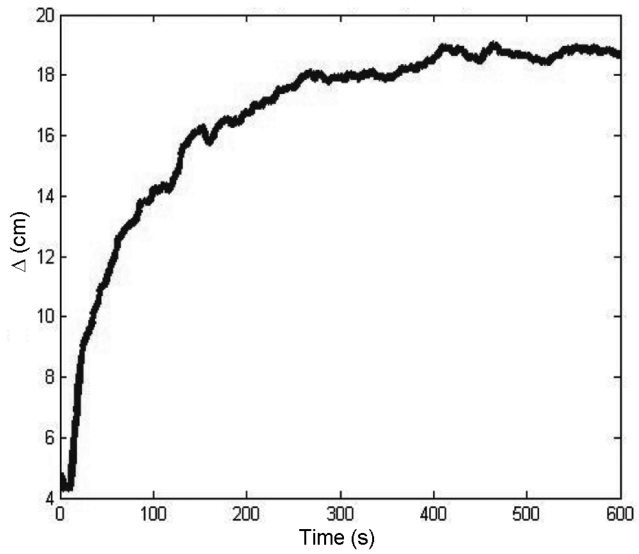

Figure 2. Evolution of the mixed layer, Δ with time.

Table 1. Experimental parameter range

Run	Q (cm^2/s^3)	Ra_f	N (s^{-1})	Ri	W (cm/s)
1	0.0076	2.58×10^7	0	0	15.01
2	0.0076	2.58×10^7	0.25	0.46	15.01
3	0.0076	2.58×10^7	0.35	1.10	15.01
4	0.0076	2.58×10^7	0.45	1.59	15.01
5	0.0076	2.58×10^7	0.55	2.56	15.01
6	0.0076	2.58×10^7	0.60	3.27	15.01
7	0.0076	2.58×10^7	0.70	4.34	15.01
8	0.0076	2.58×10^7	0.80	5.37	15.01

minutes, after which the rate declined and finally a steady mixing height was reached (Figure 2). Similarly, temperature profile also reached a steady state after the formation of a steady mixing height.

Experiments were carried out for a period of $t = 800$ s, during which the evolution of the double-diffusive convection was captured using a high-resolution camera. From trial runs it was observed that a period of 10 min was sufficient for the mixing to reach a stable state, where the mixing height does not change with time. The cooling flux, $\dot{Q}$, was maintained constant for the duration of the experiment.

Table 1 lists the various governing parameters involved. Since the cooling flux is kept constant, Ra_f and W are constant for all the runs. By changing the stratification strength, Ri was varied. The experiments were performed for lower values of N ranging from 0 (i.e. no stratification) to 0.8.

Once the cooling begins, the thermal boundary layer that develops near the tank top becomes unstable and this leads to turbulent thermal convection. Experiments were performed keeping Ra constant and varying Ri (αN^2). The results are presented for eight different Ri values (0–6) obtained for eight different stratification strengths ($N = 0$–0.8). The value of Ri was varied by changing N. Ra_f could also be varied using the cooling flux supplied at the top of the fluid layer, but in our experiments it was maintained a constant by providing a constant cooling flux $\dot{Q} \approx 1$ kW/m^2 ($Ra_f = 2.58 \times 10^7$).

When $N = 0$, the mixing layer formation is fast, and the mixing process penetrates through the fluid layer. This is mainly due to the fact that absence of buoyancy allows the temperature flux to penetrate downwards. This allows the diffusion of heat to creep into deeper fluid layers compared to the case when stratification is present. Though such a situation never occurs in the oceans, it is important to study this case as a reference for further studies. In reality, there is always stratification present in the oceans.

Figure 3 shows the mixing process for different stratification strengths. For $N = 0$, it can be clearly seen that

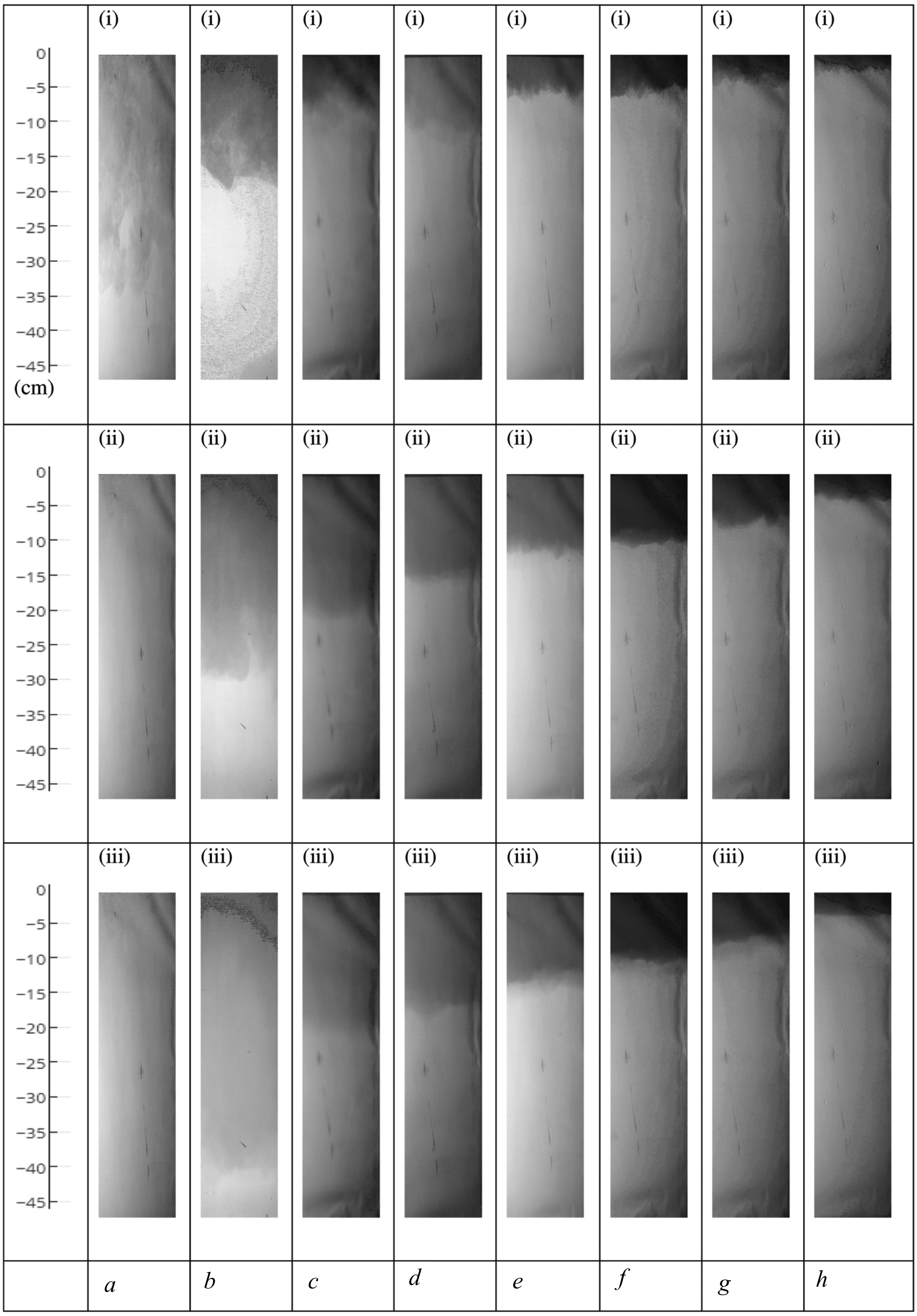

Figure 3. Mixing layer depth (cm) visualization for various stratification strengths with time. ***a–h*** represent stratification strengths 0, 0.25, 0.35, 0.45, 0.55, 0.60, 0.70, 0.80 respectively. i–iii are images at time $t = 30$, 300 and 600 sec respectively.

the mixing takes place throughout the tank as the final density and temperature values are uniform throughout the tank. This indicates that with no opposition to temperature diffusion by the buoyancy and for $N = 0$, the temperature penetrates quickly and uniformly throughout the tank thereby resulting in a deep mixed layer. The density changes from an initial value of 998 kg/m^3 to a final value of 998.8 kg/m^3 and temperature changes from an initial value of 25°C to a final value of 22.5°C. From temperature–density plot for water, a decline of 3.5°C in

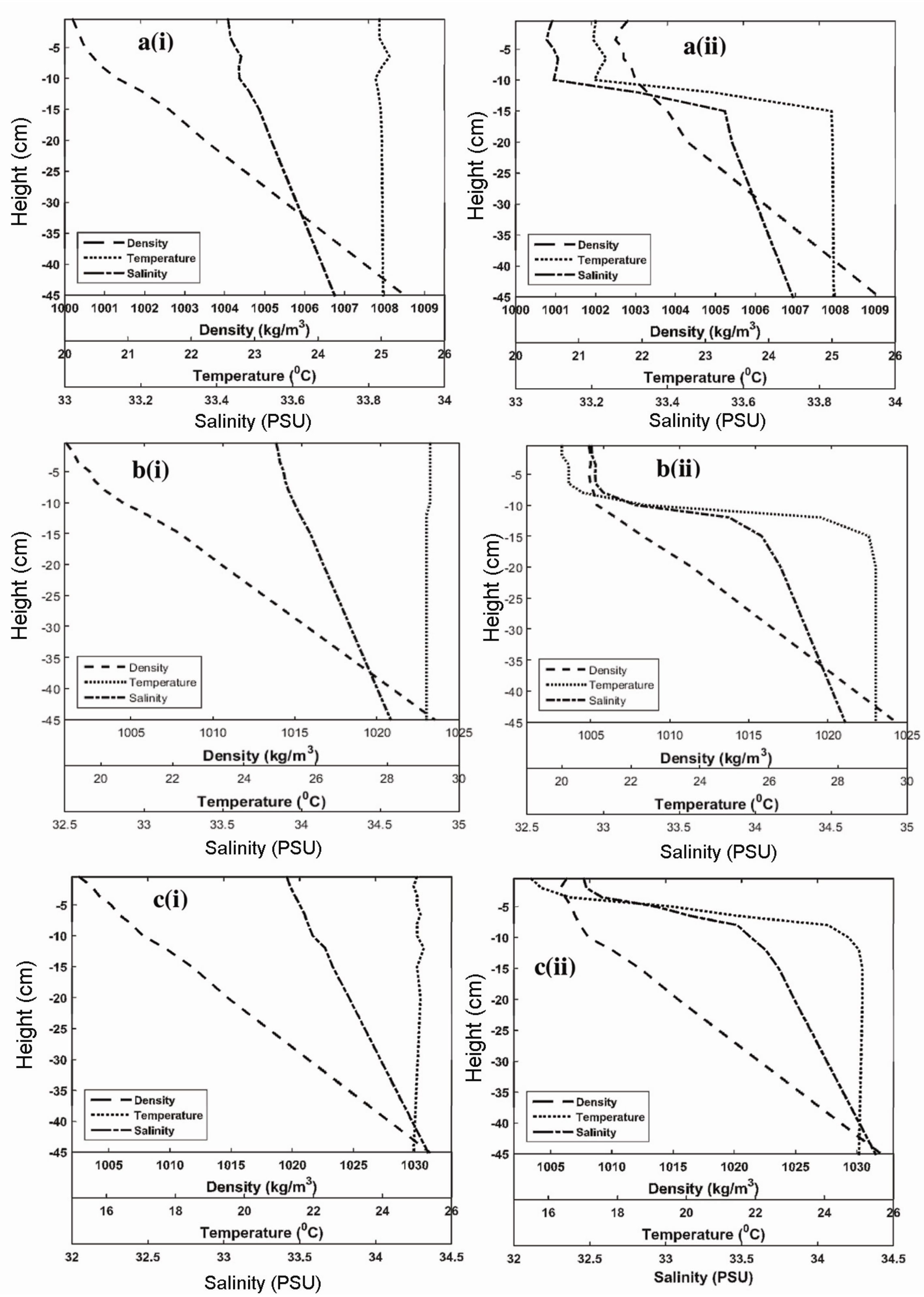

Figure 4. Temperature and salinity profiles for various stratification strengths. [a(i), a(ii)], [b(i), b(ii)] and [c(i), c(ii)] are the initial and final profiles for $N = 0.45$, 0.70 and 0.80 respectively.

temperature corresponds to 0.7–0.8 kg/m^3 increase in density. So, it can be stated that the increase in density throughout the tank is solely due to the increase in temperature. Therefore, in the absence of any stratification, the cooling flux diffuses into the entire fluid present in the tank and causes mixing in the entire tank. Now, having established a reference case for our study, further experiments with non-zero Ri were performed. In cases with non-zero Ri, it was observed that there was a distinct mixing layer at the top where all the mixing took place and the properties further below this mixing layer were unaffected. In addition, it was observed that the evolution of mixing layer for each non-zero Ri case followed $t^{1/2}$ law as proposed in eq. (1) and confirmed from Figure 2. The MLD was measured by the visualization experiments using a threshold method in MATLAB. To confirm the measurements of mixed layer thickness from the visualization experiments, vertical profiles of salinity and temperature were measured, which can be used to obtain the density using the equation of state.

The profiles were obtained by drawing a small amount of fluid at 5 mm interval, once steady state conditions were achieved. Using a high-precision densitometer and thermometer, salinity and temperature of the fluid were obtained at different vertical heights. For calculating salinity, the following equation of state was used

$$\rho = \rho_0(1 + \beta S - \alpha T),$$

where S is the salinity and T is the temperature. The constant $\alpha = 0.0034/K$ and $\beta = 0.03/S$ are coefficients of thermal expansion and salinity contraction respectively.

Figure 4 shows the initial and final profiles of ρ, T and S. As can be observed from the figure, a mixing layer (where all properties are uniform) is present in the experiments with non-zero stratification. In addition to the mixing layer where all the properties are uniform, there exists a barrier layer between the mixing layer and unmixed fluid. The barrier layer has strong property gradients. The relative strength of salinity and temperature gradients decides whether the temperature will penetrate further down in the fluid. In the barrier layer, buoyancy acts as a deterrent for the cooling flux to penetrate deeper and limits the mixing layer to a few centimetres at the top. We do not see a staircase-like profile in Figure 4, as documented by Fernando[6], due to the effect of surface cooling. Along with reduction in MLD, BLD was also reduced. That indicates that sharper gradients are present in higher Ri cases in the barrier layer. So, an increase in Ri causes an increase in the buoyancy opposition for temperature penetration in stratified fluids.

Also, for higher Ri cases the decrease in temperature in the mixing layer is around 8°–10°C while for lower Ri cases, the corresponding fall in temperature in the mixing layer is around 3°–5°C. This can be explained by the fact that with increasing Ri, MLD decreases. This shows that the cooling flux (which is constant) is getting absorbed in a smaller volume or mass of water. So, from $mC_p\Delta t = \dot{Q}\tau$ (where τ is the total time of experiment) we can conclude that for smaller m, there is higher fall in temperature (since $\dot{Q}\tau$ is constant), which is also observed here.

We have argued earlier in the text that the thickness of the convecting layer that can remain quasi-stationary should be given by eq. (7). We have checked the validity of this theoretical result by measuring Δ from experiments. The Δ values obtained from visualization and vertical profiles were in good agreement. Figure 5 shows the variation of Δ with Ri. It can be observed that MLD decreased with increase in Ri.

Using Figure 5, it is possible to evaluate the average value for $C_4 \approx 54.0$. Noting from eq. (7) that $C_4 = (C_1^2/C_2C_3)^{3/4}$ with $C_1 \approx 1$ and $C_2 \approx 0.125$ and $C_3 = (1/2 - C^{-2}) = 0.039$ (ref. 22), we obtain $C_4 \approx 54.1$, which is in good agreement with our experimental results. It should be noted that the value of C_4 is extremely sensitive to the choice of C, for which our measurements give an average value of 1.47, which is in close agreement with that reported in Fernando[6].

Apart from MLD variation with N, entrainment velocity variation was also obtained. Entrainment is the transport of fluid because of eddies that form due to the cooling flux from the top diffusing in the stratified fluid below. The entrainment velocity U_e is obtained by the time average of the rate of mixing layer evolution till the MLD reaches 99.9% of the steady-state depth.

$$U_e = \frac{1}{T}\int_0^T \frac{dh}{dt}\, d\tau,$$

where T is the time required for the MLDF to reach about 99% of the steady-state value.

With the increase in N, U_e was observed to decrease exponentially. The exponent is found –3/2 from the best-fit curve. Figure 6 represents this variation graphically.

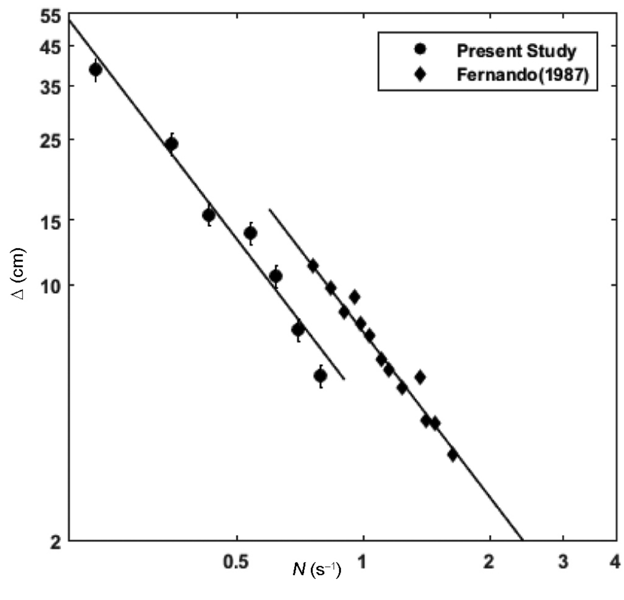

Figure 5. Variation of Δ with N at constant $Q = 0.0076$ cm^2/s^3 (present study) and $Q = 0.032$ cm^2/s^3 (ref. 6). Solid lines represent slopes of –3/2.

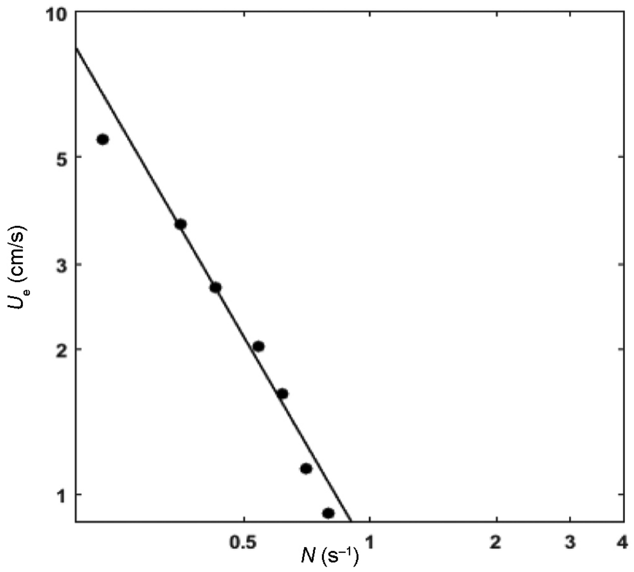

Figure 6. Entrainment velocity U_e, as a function of N. Solid line represents slope of –3/2.

An experimental study for the dependence of mixing layer thickness, on the stratification strength (which manifests itself in the form of Richardson number) and for a constant cooling flux (given by flux Rayleigh number) is presented here. When the convective layer grows to a certain size, the balance of vertical kinetic energy and the potential energy of eddies in the convecting layers determine the thickness of the mixed layer. Using this argument, Fernando[6] theoretically formulated an empirical relation for mixing layer thickness as a function of Ri and found it to vary as $Ri^{-3/4}$ (i.e. $N^{-3/2}$). The validity of this relation at weaker and moderate stratification strengths has been tested in the present study.

From both the dye visualization and vertical temperature and salinity profiles, it can be concluded that MLD decreases with increase in Ri. Further, it has been confirmed that $\Delta = \hat{C}Ri^{-3/4}$, when $N > 0$. The value of constant $\hat{C}$ was experimentally found to be ≈ 27. These findings indicate that buoyancy effects are stronger in higher Ri cases, which do not allow the temperature to diffuse deeper. The vertical profiles indicate that along with the MLD, the barrier layer also shifts upwards and shrinks with increasing Ri. This shrinkage makes the gradients sharper for higher Ri cases, thus restricting the mixing to a smaller height. An empirical relation for entrainment velocity has also been formulated ($U_e = C^*Ri^{-3/4}$). The value of constant C^* was experimentally found to be ≈ 0.74. These results have relevance to the wintertime mixing phenomenon observed in BoB.

1. Schmitt, R., W., Form of the temperature–salinity relationship in the central water: evidence for double-diffusive mixing. *J. Phys. Oceanogr.*, 1981, **11**, 1015–1026.
2. Hendricks, P. J., Muench, R. D. and Stegen, G. R., A heat balance for the Bering Sea ice edge. *J. Phys. Oceanogr.*, 1985, **15**, 1747–1758.
3. Turner, J. S. and Stommel, H., A new case of convection in the presence of combined vertical salinity and temperature gradients. *Proc. Natl. Acad. Sci. USA*, 1964, **52**, 49–53.
4. Turner, J. S., The influence of molecular diffusivity on turbulent entrainment across a density interface. *J. Fluid Mech.*, 1968, **33**, 639–656.
5. Huppert, H. E. and Linden, P. F., On heating a stable salinity gradient from below. *J. Fluid Mech.*, 1979, **95**, 431–464.
6. Fernando, H. J. S., The formation of a layered structure when a stable salinity gradient is heated from below. *J. Fluid Mech.*, 1987, **182**, 525–541.
7. Kerpel, J., Tanny, J. and Tsinober, A., On a stable solute gradient heated from below with prescribed temperature. *J. Fluid Mech.*, 1991, **223**, 83–91.
8. Guo, Shuang-Xi, Zhou, Sheng-Qi, Qu, Ling and Lu, Yuan-Zheng, Laboratory experiments on diffusive convection layer thickness and its oceanographic implications. *J. Geophys. Res.: Oceans*, 2016, **121**, 7517–7529.
9. Kelley, D. E., Effective diffusivities within oceanic thermohaline staircases. *J. Geophys. Res.*, 1984, **89**, 10484–10488.
10. Konstantin, F. N., Layer thicknesses and effective diffusivities in diffusive thermohaline convection in the ocean. *Elsevier Oceanogr. Ser.*, 1988, **46**, 471–479.
11. Rao, R. R., Molinari, R. L. and Festa, J. F., Evolution of the climatological near-surface thermal structure of the tropical Indian Ocean: 1. Description of mean monthly mixed layer depth, and sea surface temperature, surface current, and surface meteorological fields. *J. Geophys. Res.: Oceans*, 1989, **94**, 10801–10815.
12. Zhou, S.-Q. *et al.*, New layer thickness parameterization of diffusive convection in the ocean. *Dyn. Atmos. Oceans*, 2016, **73**, 87–97.
13. Bergman, T. L., Incropera, F. P. and Viskanta, R., A differential model for salt-stratified, double-diffusive systems heated from below. *Int. J. Heat Mass Transf.*, 1985, **28**, 779–788.
14. Newman, F. C., Temperature steps in Lake Kivu: a bottom heated saline lake. *J. Phys. Oceanogr.*, 1976, **6**, 157–163.
15. Veronis, G., On finite amplitude instability in thermohaline convection. *J. Mar. Res.*, 1965, **23**, 1–17.
16. Deardorff, J. W., Willis, G. E. and Stockton, B. H., Laboratory studies of the entrainment zone of a convectively mixed layer. *J. Fluid Mech.*, 1980, **100**, 41–64.
17. Hunt, J. C. R., Turbulence structure in thermal convection and shear-free boundary layers. *J. Fluid Mech.*, 1984, **138**, 161–184.
18. Long, R. R., A theory of mixing in a stably stratified fluid. *J. Fluid Mech.*, 1978, **84**, 113–124.
19. Howden, S. D. and Murtugudde, R., Effects of river inputs into the Bay of Bengal. *J. Geophys. Res.: Oceans*, 2001, **106**, 19825–19843.
20. Vecchi, G. A. and Harrison, D. E., Monsoon breaks and subseasonal sea surface temperature variability in the Bay of Bengal. *J. Climate*, 2002, **15**, 1485–1493.
21. Oster, G. and Yamamoto, M., Density gradient techniques. *Chem. Rev.*, 1963, **63**, 257–268.
22. Fernando, H., J. S. and Long, R. L., On the nature of the entrainment interface of a two-layer fluid subjected to zero-mean-shear turbulence. *J. Fluid Mech.*, 1985, **151**, 21–53.

Received 23 May 2017; revised accepted 30 November 2017

doi: 10.18520/cs/v114/i09/1953-1960